HHS Public Access

Author manuscript

Brain Struct Funct. Author manuscript; available in PMC 2019 June 01.

Published in final edited form as:

Brain Struct Funct. 2018 June ; 223(5): 2343–2360. doi:10.1007/s00429-018-1635-z.

Tinnitus and temporary hearing loss result in differential noise-induced spatial reorganization of brain activity

Antonela Muca[1], **Emily Standafer**[1], **Aaron K. Apawu**[1], **Farhan Ahmad**[1], **Farhad Ghoddoussi**[2], **Mirabela Hali**[1], **James Warila**[1], **Bruce A. Berkowitz**[1,3], and **Avril Genene Holt**[1,4]

[1]Department of Anatomy and Cell Biology, Wayne State University School of Medicine, 550 East Canfield Ave., Detroit, MI 48201, USA

[2]Department of Anesthesiology, Wayne State University School of Medicine, Detroit, MI, USA

[3]Department of Ophthalmology, Wayne State University School of Medicine, Detroit, MI, USA

[4]John D. Dingell VAMC, Detroit, MI, USA

Abstract

Loud noise frequently results in hyperacusis or hearing loss (i.e., increased or decreased sensitivity to sound). These conditions are often accompanied by tinnitus (ringing in the ears) and changes in spontaneous neuronal activity (SNA). The ability to differentiate the contributions of hyperacusis and hearing loss to neural correlates of tinnitus has yet to be achieved. Towards this purpose, we used a combination of behavior, electrophysiology, and imaging tools to investigate two models of noise-induced tinnitus (either with temporary hearing loss or with permanent hearing loss). Manganese (Mn^{2+}) uptake was used as a measure of calcium channel function and as an index of SNA. Manganese uptake was examined in vivo with manganese-enhanced magnetic resonance imaging (MEMRI) in key auditory brain regions implicated in tinnitus. Following acoustic trauma, MEMRI, the SNA index, showed evidence of spatially dependent rearrangement of Mn^{2+} uptake within specific brain nuclei (i.e., reorganization). Reorganization of Mn^{2+} uptake in the superior olivary complex and cochlear nucleus was dependent upon tinnitus status. However, reorganization of Mn^{2+} uptake in the inferior colliculus was dependent upon hearing sensitivity. Furthermore, following permanent hearing loss, reduced Mn^{2+} uptake was observed. Overall, by combining testing for hearing sensitivity, tinnitus, and SNA, our data move forward the possibility of discriminating the contributions of hyperacusis and hearing loss to tinnitus.

Keywords

Tinnitus; Hyperacusis; Neuronal activity; Hyperactivity; Neuroplasticity; Hearing loss; Permanent threshold shift; Temporary threshold shift; Manganese enhanced MRI; Gap detection; MEMRI; Acoustic startle reflex

Avril Genene Holt, agholt@med.wayne.edu.

Introduction

Chronic tinnitus, the perception of a ringing, buzzing or hissing sound in the absence of an external stimulus, affects approximately 15% of the population. Tinnitus is most prevalent in older individuals and those constantly exposed to loud noise and is on the rise in adolescents (Shargorodsky et al. 2010; McCormack et al. 2016). Although chronic tinnitus can have a negative impact on quality of life, mental health, and auditory function there are few techniques that allow objective diagnosis or mapping of the biological effects of tinnitus in vivo. As such, the underlying mechanisms of tinnitus are still not well understood. The result of which is that there are no reliable and effective treatments for tinnitus (Jastreboff and Hazell 1993; Lockwood et al. 1998).

Studies have suggested that both increases and decreases in spontaneous neuronal activity (SNA) occur in tinnitus models (e.g., Kaltenbach et al. 2005; Brozoski et al. 2007; Auerbach et al. 2014; Ropp et al. 2014). Changes in spontaneous neuronal activity (SNA) in auditory-related brain regions [e.g., cochlear nucleus (CN), the inferior colliculus (IC), and the auditory cortex (AC)] have been suggested as a biomarker of tinnitus (Baizer et al. 2012; Brozoski et al. 2002, 2007; Eggermont and Roberts 2004; Holt et al. 2010; Kaltenbach et al. 2005; Mulders and Robertson 2013; Robertson et al. 2013; Shore et al. 2007). However, there has not been a consensus on when or which brain region to focus on to study SNA changes after the onset of noise-induced tinnitus. Several approaches have been employed to define temporal and spatial tinnitus-related changes in SNA, for example, studies are often performed in tissue slices (Basta and Ernest 2004), ex vivo (Brozoski et al. 2010, 2013), or in anesthetized animals (Brozoski et al. 2002; Robertson et al. 2013; Mulders and Robertson 2013). The results point to the necessity of refining and utilizing methods for in vivo evaluation of changes in SNA concurrently across multiple auditory-related brain regions. Thus, studying neuronal plasticity associated with noise-induced tinnitus remains problematic, but is important to elucidate in order to identify types and windows of therapeutic intervention.

One method that can be used to address this problem is manganese enhanced MRI (MEMRI). Manganese (Mn^{2+}) is a calcium ion surrogate (and MRI contrast agent) that readily enters active neurons while the animal is awake and behaving. Manganese uptake can occur within hours via L-type calcium channels. Because efflux of Mn^{2+} is much slower (days to weeks), Mn^{2+} levels within brain regions represent an index of SNA, which primarily correlated with the time of manganese administration (Salvi and Arehole 1985; Takeda 2003). Importantly, encoding SNA using manganese occurs while the animal is awake and freely moving, although the measure of the encoded signal using manganese-enhanced MRI (MEMRI) requires anesthetizing the animal. Encoding SNA in the awake and freely moving animal offers a major advantage of allowing potentially confounding influences of ambient and scanner noise to be minimized. Therefore, MEMRI is the imaging modality of choice for measuring neuronal activity throughout the auditory pathway with high spatial resolution in awake and freely moving animals (Silva and Bock 2008; Cacace et al. 2014).

Also, the contribution of hearing status to tinnitus effects is not well understood. In addition, we also find that GAP inhibition of the acoustic startle reflex (GAP) is a powerful non-invasive approach for studying tinnitus. GAP detection is a behavioral test for tinnitus that examines the ability to discriminate a gap of silence embedded in a carrier tone of a specific frequency and intensity. Subjects hearing both the carrier tone and the silent gap have a reduced response to a loud startle sound presented after the gap of silence. If the silent gap is obscured by the subject's tinnitus (similar frequency and intensity) the startle response is more similar to the condition in which there is no gap of silence preceding the startle sound. This deficit in GAP detection has been correlated with tinnitus (Campolo et al. 2013; Galazyuk and Hébert 2015; Holt et al. 2010; Lobarinas et al. 2013; Turner et al. 2006; Turner and Larsen 2016).

We have already demonstrated MEMRI and GAP detection to be useful in the study of noise- and drug-induced tinnitus during acute the stages of the condition (Holt et al. 2010). Whether MEMRI and GAP detection will be useful at longer times after tinnitus onset remains to be determined. In the current study, we tested the hypothesis that the central effects of hearing loss are distinguishable from the effects of tinnitus 2 months after noise exposure. Manganese uptake was used as representative of neuronal activity with hearing status and tinnitus examined by auditory brainstem response (ABR), pre-pulse inhibition, and GAP inhibition of the acoustic startle reflex. Two animal models were employed to test the hypothesis (Brozoski et al. 2007; Heffner and Harrington 2002; Turner et al. 2006), one with a permanent threshold shift (PTS) following a noise exposure and another model with a noise-induced temporary threshold shift (TTS).

Materials and methods

Subjects and design

Fifteen adult male Sprague Dawley (SD) rats were obtained from Charles River Laboratory. All rats weighed 350–380 g at the beginning of the experiment. They were individually housed and maintained at 25 °C with a 12 h light/dark cycle (lights on at 7 AM). Standard housing conditions with free access to normal rat chow and tap water were provided. Wayne State University (WSU) maintains AAALAC accredited animal facilities under the Division of Laboratory Animal Resources. Animals were treated in accordance with the Animal Welfare Act and DHHS "Guide for the Care and Use of Laboratory Animals". and all procedures were approved by the Wayne State University Institutional Animal Care and Use Committee (IACUC) in accordance with NIH guidelines.

Rats were divided randomly into three experimental groups: (1) a control group (control) exposed only to ambient noise conditions and either a (2) mild (TTS) or (3) severe group (PTS) exposed to one of two types of noise exposure (described in "Noise exposures" section). Before and after noise exposure, hearing thresholds were tested using ABR in a subset of animals (to minimize anesthesia effects). In addition, pre-pulse inhibition was used to test hearing in all animals and GAP detection was also tested for a period of eight weeks after noise exposure. Neuronal activity was assessed using MEMRI (Fig. 1).

To obtain a representative hearing threshold for each group, ABR testing was performed for at least two animals in each group with three time points assessed before and after noise exposure, and after MEMRI. Animals were anesthetized with a mixture of ketamine and xylazine (75 and 8 mg/kg i.m., respectively) and placed in a sound attenuating booth. Sub-dermal electrodes were inserted behind the ipsilateral pinna (reference electrode), on top of the head (active electrode), and behind the contralateral pinna (ground electrode). A speaker (modified Beyer) was placed into one external ear canal and 5 millisecond tone bursts were played during 1024 trials for each sound intensity level tested across three frequencies (4, 12, and 20 kHz) in increments of 5 or 10 dB from 100 to ~20 dB SPL. Evoked potentials were recorded, amplified, and filtered using Daqarta (Data AcQuisition And Real-Time Analysis) digital signal processing software (Daqarta 4.0 Ann Arbor, MI, USA). Hearing thresholds were obtained for each frequency by determining the lowest intensity at which a given tone evoked a measurable wave I response.

Acoustic startle reflex (ASR) testing

Inhibition of the ASR was measured repeatedly to determine baseline and post noise exposure responses. While in a sound attenuating booth, animals were placed in a plexiglass box with an adjustable ceiling positioned just above the back to restrict excessive movement and direct force downward onto a piezoelectric plate. Speakers were placed at the top of the sound chamber, approximately 15 cm above each animal. The output of the piezo transducer was amplified, filtered, and the root mean square of the waveform measured to determine startle amplitude. Responses were recorded using customized hardware and software (Kinder Scientific, Poway, CA, USA).

For each animal, pre-pulse inhibition (PPI) was tested first, followed by Gap inhibition (GAP) of acoustic startle. Testing lasted no longer than one hour per day. During PPI testing (Fig. 2a), pre-startle tones were presented at 4, 8, 12, 16, 20, and 24 kHz at levels equivalent to 45 and 60 dB sound pressure level (SPL) for each animal. Each pre-startle tone was presented for 50 ms in a silent background 50 ms before the startle noise (120 dB broad band noise for 20 ms). Trials of “sound off” startle noise were also played without a pre-pulse tone to determine a maximum startle response. During each session, animals completed sound off startle trials as well as trials of pre-pulse tests at each frequency and intensity for a total of 229 trials presented in random sequence. Inter-trial intervals varied between one and six seconds.

During GAP testing (Fig. 2c–e), carrier tones of 4, 8, 12, 16, 20, and 24 kHz at 45 and 60 dB SPL were presented. A silent gap lasting 50 ms was embedded in the tone 50 ms prior to the startle noise (120 dB broad band noise for 20 ms). GAP testing includes startle responses to the silent GAP in tone trials (“gap in”; $n = 108$ trials), carrier tone trials with no silent GAP included—carrier tone only—(“sound on” startle; $n = 108$ trials), trials with no sound before the startle (“sound off” startle; $n = 108$ trials), and trials with no sound and no startle ($n = 15$ trials) for a total of 339 trials.

Noise exposures

One ear in each animal was selected randomly to be blocked in order to attenuate the effects of noise and allow ASR testing. This was accomplished by inserting an industrial foam earplug (Howard Leight, Max Foam) into one ear canal. In addition, the pinna was folded over the ear canal entrance, covered with gauze, and animals were fitted with plastic collars to prevent removal during the noise exposure. Animals were then placed in individual wire mesh cages positioned on open racks in a custom-built noise exposure booth. Noise was generated using DaqGen software (Daqarta, Interstellar Research) channeled through 16 overhead speakers and Grass preamplifiers. For the TTS noise exposure group, animals were exposed to a 16 kHz, 106 dB SPL octave band noise for one hour. For the PTS noise exposure group, animals were exposed to a 10 kHz, 118 dB SPL one-third octave band noise for four hours. Octave band refers to frequency band in which the highest frequency is twice the lowest frequency whereas, in one-third octave band noise the highest frequency of the band is cubic root of 2 times the lowest frequency.

Manganese enhanced magnetic resonance imaging (MEMRI)

All rats received systemic administration of Mn^{2+} (66 mg/ kg $MnCl_2 \cdot 4H_2O$, i.p.; dissolved in saline) one hour after noise exposure, but 24 h before neuroimaging, as previously described (Holt et al. 2010). Immediately before the MRI examination, rats were anesthetized via inhalation of 5% isoflurane mixed with room air for induction, until loss of the toe-pinch reflex and then maintained on 1.5–2% isoflurane for the duration of experiment (~ 30 min). Animals were transferred to the scanner platform with a built-in, recirculating heated water system to maintain body temperature. The animal's head was stabilized using blunted ear-bars and a bite-bar.

Scans were performed on a 7 T Bruker ClinScan system with a Siemens console (for details of imaging methods see Bissig and Berkowitz 2009 and 2011). Briefly, a transmitonly whole body coil and a receive-only surface coil, placed dorsal to the head of the animal, were used to acquire two types of images based on a turbo-FLASH sequence: Scans acquired both with and without a slice-selective inversion pulse, generated magnetization prepared rapid acquisition gradient echo (MPRAGE) and proton density gradient echo weighted (PDGE) images sharing most parameters (flip angle of 3°; TE 3.03 ms; NA 1; echo spacing 7.77 ms; matrix size 192 × 192 × 112; FOV 2.50 × 2.50 × 2.91 cm^3; providing a resolution of 130 μm × 130 μm × 260 μm). The resulting scans contained a stack of 112 images spanning the brain from the caudal olfactory bulb to the caudal brainstem. For each rat the pulse sequence for collection of MPRAGE and PDGE images was executed twice. Following the scan, animals were allowed to recover from the anesthesia in a warm, clean cage without bedding.

Data analysis

ABR

For hearing thresholds, the lowest thresholds for a response to tone pips were compared across frequencies and groups using an analysis of variance. The amplitude of wave one (contribution of the auditory nerve) was compared across groups, at 12 and 20 kHz 2 days and 2 months after the exposure. The peak of wave one (P1 μV) was subtracted from the

trough of wave one (N1 μV) for each sound level tested (25–80 dB SPL). StatView (version 5.0 SAS) was used for between group comparisons to determine significant differences ($p \leq 0.05$) between experimental groups and a Scheffe test was performed for post hoc comparisons.

ASR

During ASR testing, animals had to exhibit a robust startle reflex in response to the startle stimulus, as well as attenuate the startle reflex in the presence of a pre-pulse or a silent gap embedded in a tone in order to be included in the study. During each ASR trial, the startle force exhibited by the animal had to be at least 50 times greater than the force exhibited by standing/walking only. Pre-pulse and GAP trials with changes greater than 200% (excessive movement) or less than 10% (very little startle) were excluded from analysis. If more than 50% of trials were removed for any frequency then the entire session was excluded from analysis. If more than 50% of the sessions were excluded then the animal would be removed from the study.

For PPI, results were calculated as the force of the startle response elicited in response to the startle noise when preceded by the pre-pulse, divided by the response to the startle noise alone. For GAP detection, the data were calculated in the same way except that: (1) the pre-pulse was replaced by a gap of silence for each trial at each frequency and sound level, (2) the maximum startle response was also recorded in the presence of the background tone. Data were analyzed similarly using StatView (version 5.0 SAS) for betweengroup comparisons and within-group comparisons to determine significant differences between and across frequencies with Tukey tests performed for post hoc comparisons.

In addition, *GAP detection* is defined as when the startle response following a GAP of silence in the tone, is less than the maximum startle response with no tone present (Fig. 2d). This is usually under normal conditions—the control group. *Reduced GAP detection* is when the startle response following a GAP of silence in the tone, is closer to the maximum startle response—increased startle (Fig. 2e). This is what we associate with tinnitus. *Enhanced GAP detection* is when the startle response following a GAP of silence in the tone, is much less than the maximum startle response when there is no tone present—decreased startle. This is associated with a “hyperacusis-like” circumstance.

MEMRI

Normalization Differences in Mn^{2+} uptake across conditions and regions result from measurement of tissue T1 values and reflect signal intensity from regions of interest within the image. Since several other factors may affect signal intensity measured in standard T1-weighted images, such as tissue proton density, distance from receive-coil, and B1 inhomogeneity (Chuang et al. 2009) normalization is required. Because gradient echo images (PDGE and MPRAGE) acquired with a small flip angle would share the influence of these possible scanner artifacts, a ratio image (MPRAGE/ PDGE) can be created that is weighted heavily by tissue T1 and largely free of the afore mentioned non-biological influences on signal (Van de Moortele et al. 2009). In addition, all functional comparisons of MEMRI data, brain signal intensities were normalized to muscle, similar to the approach we

have previously used (Bissig and Berkowitz 2014; Holt et al. 2010). Muscle normalization compensates for signal intensity gradients that remain after image processing and potential inter-individual differences in peripheral $MnCl_2$ administration and uptake (e.g. liver sequestration).

Using our established analysis protocol (Bissig and Berkowitz 2014), the two stacks of MPRAGE images from each animal were imported into Image J (NIH Bethesda, MD) and signal intensity was added on a voxel-by-voxel basis to produce a MPRAGE_sum image. Similar steps were repeated for the two stacks of PDGE images to produce a PDGE_sum image.

Using the in-house developed R language scripts (v.2.9.0, R Development Core Team, 2009; http://www.R-project.org), the number of the slices in both the MPRAGE_ sum and PDGE_sum images was doubled from 112 to 224 with the thickness of each image slice decreased from 260 to 130 μm, by inserting a duplicate slice adjacent to each original slice. This allowed a symmetric cube 130 μm on each side to be produced instead of the original 130 μm × 130 μm × 260 μm rectangle produced originally. Next, the ratio of the signal intensity of the modified MPRAGE_sum and PDGE_sum images were calculated on a voxel by voxel basis to produce the T1 weighted image (T1w_ratio).

For each rat, the T1w_ratio image stack was used for quantification of regions of interest (ROIs) by importing the stack to MRIcro v.1.40 (Rorden and Brett 2000). Neuroanatomical landmarks and a rat brain atlas (Paxinos and Watson 2007) were used to define ROIs. Each anatomical region was identified by shape, size, and proximity to prominent adjacent structures. For tonotopic analysis within the CNIC, four parallel bands were delineated. The most dorso-lateral bands were defined as the lowest frequency regions and the most ventro-medial regions were defined as the highest frequency regions. Each hand-drawn ROI was placed in two to four 130 μm slices spanning the rostro-caudal extent of each brain region with the defined region drawn to occupy the entire coronal profile of each nucleus, excluding a border buffer of approximately one voxel wide depending on the ROI. Appropriate ROI placement was confirmed in parasagittal views and the subject-to-subject consistency of ROI placement was verified by at least two of the authors.

The average signal intensity was measured from each ROI including several midbrain and brainstem regions: the central nucleus, dorsal cortex, and external cortex of the inferior colliculus (CNIC, DCIC and ECIC, respectively), the dorsal (DCN) and ventral (VCN) cochlear nucleus, the paraflocculus (PFL), the superior olivary complex (SOC) and medial geniculate body (MGB). Several cortical regions, both traditionally auditory–primary auditory cortex (Au1), dorsal zone of auditory cortex (AuD), and ventral zone of auditory cortex (AuV), as well as regions not traditionally associated with auditory pathways - temporal association area (TeA) and hippocampus (CA1) were also investigated. The combination of four regions, TeA, AuV, Au1 and AuD, was labeled Auditory Cortex (AuC) and was examined as a group. In addition, average signal intensity was collected for muscle.

Results

ABR

Sound exposure results in PTS, TTS, and modulated wave I amplitudes—After the noise exposure, both the 12 and 20 kHz frequencies were significantly affected for the PTS and TTS groups (Table 1). Animals exposed only to ambient noise levels (control) had hearing thresholds averaging 33.2 ± 0.8 dB.

The PTS noise exposure group demonstrated elevated thresholds similar to that in our previous report (Holt et al. 2010) in both the unprotected (62.7 ± 1.3 dB) and protected ear (51.5 dB ± 0.16) 2 days after the noise exposure. The TTS noise exposure group exhibited elevated thresholds in the unprotected ear (42.7 dB ± 1.2) while the protected ear was not significantly different from controls (33.2 ± 0.8) 2 days following noise exposure (Fig. 3a, b). In both the PTS and TTS groups the non-protected ear exhibited the highest thresholds at 2 days (Fig. 3a). Two months after noise exposure, the unprotected ear from animals in the TTS noise exposure group (36.0 ± 1.2) had hearing thresholds that were not significantly different from that of the control group (33.5 ± 0.6 dB). However, the unprotected ear from animals in the PTS noise exposure group had thresholds that were elevated 26% ($p \leq 0.05$) above the control group and 20% ($p \leq 0.05$) above that of the TTS noise exposure group (Fig. 3a). By 2 months, hearing thresholds in the protected ear from animals in both the TTS and PTS groups had returned to normal (Fig. 3b).

Noise exposure results in long-term changes in ABR wave I amplitude—Both at 2 days and 2 months following noise exposure the contribution of the vestibulo-cochlear nerve to the ABR was assessed by comparing the amplitude of wave I across groups in the non-protected ear. At 12 kHz, there were no significant changes in wave I amplitude at 70 or 80 dB SPL in the PTS or TTS group when compared to the control group 2 days after noise exposure (Fig. 3c). There was also no significant difference in wave I amplitude 2 days after noise exposure at 20 kHz for either the PTS or TTS group when compared to the control group at 70 or 80 dB SPL (Fig. 3**e**). Two months after the noise exposure, there was no significant difference in wave I amplitude at 12 kHz (Fig. 3d) between the PTS and the TTS groups at 70 or 80 dB SPL when compared to the control group ($p \leq 0.60$ for each). However, at 20 kHz, after 2 months, while there was only a trend toward increased wave I amplitudes in the PTS group at 80 dB SPL when compared to controls ($p = 0.073$), amplitudes in the TTS group were significantly elevated at 80 dB SPL ($p = 0.047$) by almost four times when compared to the control group (Fig. 3f).

Noise exposure results in ASR deficits regardless of hearing threshold—To determine whether changes in ABR threshold and wave I amplitude interfered with the ability to startle, we examined performance during ASR testing.

Pre-pulse inhibition—Data are reported as percentage of maximum startle, where the maximum is 100% (*y*-axis). Thus, the smaller the percentage of maximum startle, the more the startle response is reduced (the better the performance).

All subjects were able to respond to the pre-pulse with a reduction in maximum startle response during PPI ASR testing both before and after noise exposure (Fig. 4). In the control group, the mean reduction in startle was 40% during collection of baseline values and 55% during the subsequent eight weeks. Similarly, in the TTS group, the initial reduction in startle was 43.2 and 51.9% after the noise exposure.

In the severe noise group, the initial startle reduction was 38.2 and 32.2% after noise exposure that produced a PTS (Fig. 4). These results indicate that animals were capable of hearing the pre-pulse across frequencies tested and hearing the tone during GAP testing.

GAP detection—As with PPI, data are reported as percentage of maximum startle (100%, *y*-axis). Therefore, the smaller the percentage of maximum startle, the more the startle response is reduced (the better the performance). During GAP detection testing, animals in each group demonstrated reduced startle in response to a gap of silence prior to the startle noise, across all tested frequencies before noise exposure (control − 29.6% ± 1.3; PTS − 24.6% ± 1.0; TTS − 28.7% ± 1.2). Noise exposure, did not significantly diminish the startle in response to a gap of silence prior to the startle noise, with animals displaying startle responses reduced by at least 25%. Specifically, the control group exhibited startles reduced by 32.6% ± 0.87, 26.7% ± 0.84 by the PTS group, and 35.2% ± 0.87 by the TTS group (Fig. 5).

GAP detection across groups—There were no significant differences in baseline startle at either 12 or 16 kHz across groups. After the noise exposure, GAP detection irregularities were noted in each group at 12 kHz (a), 16 kHz (b), and in individual animals at 24 kHz (data not shown). In the first week after the noise exposure, GAP detection in the TTS group was significantly enhanced at 12 kHz by 22% when compared to the control and PTS groups (Fig. 6a). By week 2, this enhanced startle reduction in the TTS group reverted to response levels that were similar to those observed during baseline testing, with no significant differences between groups. During the second month, while there was a trend towards reduced GAP detection in the TTS group, the startle response was not significantly different from the control group ($p \leq 0.06$). However, the PTS group demonstrated a significant reduction (42%) in GAP detection at 12 kHz (Fig. 6a). At 16 kHz, enhanced GAP detection (29%) was observed for the TTS group during the two-four week time point (Fig. 6b). Just as at 12 kHz, GAP detection deficits were present in the PTS group at the 5–8 week time point when compared to TTS and control groups (Fig. 6b). This trend held true at 24 kHz for 25% of animals in the PTS group (data not shown).

MEMRI

Noise exposure results in differential manganese uptake in auditory-related brain regions.—When we collated data across all of the auditory-related brain regions that were examined, both the PTS and TTS groups demonstrated significantly less Mn^{2+} uptake ($p < 0.0001$ and $p < 0.0048$, respectively) than the control group (Fig. 7). The PTS group had the least manganese uptake across groups.

In manganese uptake were observed in three brain regions (DCN, IC, and AC) when compared to controls 2 months after noise exposure. Neurons in the DCN had reduced Mn^{2+}

uptake after noise exposure with a significant reduction ($p \leq 0.05$) in the PTS group compared to the control group (Fig. 8). The DCN from the TTS group was not significantly different from the DCN of either the control or PTS group. The DCIC neurons from the PTS group had significantly reduced Mn^{2+} uptake when compared to DCIC neurons from the control group ($p < 0.05$), but were not significantly different from the DCIC neurons from the TTS group (Fig. 9b).

While the CNIC as a whole reflected no change in Mn^{2} uptake regional differences were observed (Fig. 9a). Four medio-lateral areas of the CNIC were compared from dorsal to ventral (Fig. 9a). In the PTS group, there was a significant decrease in Mn^{2+} uptake in the more dorsal regions of the contralateral CNIC (p values from most ventral—to most dorsal = 0.162 V2; 0.038 V1; 0.016 D2; 0.040 D1) when compared to controls (Table 2). Significant differences in Mn^{2+} uptake after noise exposure were also found in the DCIC (Fig. 9b).

Neurons from the auditory cortex exhibited differential Mn^{2+} uptake depending on the group from which they were sampled (Fig. 10). On average, AC neurons from the control group had higher Mn^{2+} uptake compared with either the TTS or PTS groups. Once again Mn^{2+} uptake was lowest in neurons from the PTS group ($p < 0.05$). While the uptake of Mn^{2+} in the AC from the TTS group was diminished, it was not significantly different from either the control or the PTS group.

We also compared the of Mn^{2+} uptake across brain regions in the central auditory pathway within each group (control, TTS, and PTS) to determine how noise exposure affects the neuronal activity profile across brain regions. The lowest levels of uptake were consistently observed in the AC and the medial geniculate body of the thalamus (Fig. 11). In the control group, the highest level of Mn^{2+} uptake was observed in the DCN followed by the SOC. In contrast, for the TTS and PTS groups the SOC showed the highest level of Mn^{2+} uptake followed by the DCN and VCN. Interestingly, subdivisions of the IC have different levels of manganese uptake depending upon noise exposure status. In the normal hearing, non-noise exposed group, the DCIC exhibited the highest level of manganese uptake, but in the PTS group the DCIC had the least amount of uptake of the IC subdivisions. Even in the TTS group, when hearing thresholds were normal, the DCIC had relatively less Mn^{2+} uptake than in the control group, but still higher than other IC subdivisions. Interestingly, 2 months following a PTS the ECIC and the CIC appear to show a general shift towards increased Mn^{2+} uptake (Fig. 11).

Discussion

Noise exposures, even those that do not result in permanent hearing loss, have chronic effects on neuronal activity, even 2 months after trauma. After a single exposure to a loud noise producing either a permanent or a temporary hearing loss, we have demonstrated (1) PTS-related GAP detection deficits with decreases in manganese uptake in the cochlear nucleus, inferior colliculus, and auditory cortex; (2) increased ABR wave I amplitude and enhanced GAP detection (ASR inhibition) following TTS and (3) reorganization of spontaneous manganese uptake in the auditory pathway after both PTS and TTS.

GAP inhibition of ASR is differentially affected by PTS and TTS—The acoustic startle reflex encompasses a neural circuit involving brainstem and spinal neurons (Davis 1984; Koch 1999). The ASR can be attenuated with a pre-pulse of noise or a gap of silence preceding the startle sound, which further involves midbrain and thalamic neurons (Swerdlow et al. 2001; Carlson and Willott 1996; Turner et al. 2006). This reduction of ASR is believed to result from sensory input regulated by central inhibitory processes and thus provides a means to discriminate hearing sensitivity at or above threshold (Young and Fechter 1983; Carlson and Willott 1996; Ison and Allen 2003). In the current study hearing thresholds were tested with ABR and more frequently with pre-pulse inhibition of ASR to permit assessment of peripheral hearing loss as a factor during GAP detection performance. This is important because studies have shown that while profound deafness may affect performance during GAP detection, preserving hearing in at least one ear, as in the current study, allows retention of the ability to hear the tones used during PPI sessions and is sufficient for reliable performance during GAP inhibition of ASR testing (Longenecker et al. 2014; Longenecker and Galazyuk 2011, 2012; Turner et al. 2006). Prior to noise exposure, animals in all groups exhibited reduced startle responses when a short duration tone preceded the startle noise during PPI sessions. Two months following a TTS or PTS noise exposure, there were no significant changes in the degree of pre-pulse startle inhibition, indicating that animals in both groups were able to detect tones presented during PPI testing. These results, similar to other studies, suggest that hearing was adequate for normal performance during GAP detection testing (Hickox and Liberman 2014; Holt et al. 2010; Knipper et al. 2013; Longenecker and Galazyuk 2012; Turner and Parrish 2008).

The results from our noise exposure groups are similar to other studies that reported GAP detection deficits after severe noise trauma and GAP detection enhancements after mild noise trauma. Deficits in GAP detection-reduced startle inhibition have been correlated with tinnitus (Turner and Larsen 2016; Turner and Parrish 2008). The premise is that tinnitus interferes with processing of the silent gap, typically resulting in a startle response that is less attenuated.

Enhanced startle inhibition has been associated with early postnatal noise exposures (Rybalko et al. 2011). They report that startle inhibition strength increases with increased sound intensity. However, after early postnatal noise exposure maximum startle inhibition occurs at lower intensities and is similar to that of the higher intensities observed in littermate controls. This complements our current results of increased startle inhibition at (16 kHz) and near (12 kHz) the noise exposure frequency and increased ABR wave I amplitude in the TTS group at 20 kHz, a frequency that is above that of the noise exposure (16 kHz). Mild noise exposure often results in augmented gain in neurons with characteristic frequencies above the noise exposure frequency (Hickox and Liberman 2014). Thus results from the current study suggest that intensity levels in the TTS group are experienced as louder than the same level in the control group.

These results suggest that factors such as modulation of the gain of central auditory neurons may be at play, with exposure to loud noise resulting in an increased sensitivity to sound even as much as one month later (Fig. 3). This change in ASR sensitivity has been referred to as hyperacusis. Previous studies suggest caution in using the term hyperacusis, typically

used clinically to denote heightened awareness, hypersensitivity, discomfort, hyper-responsiveness, intolerance, or irritability in response to sound (Tyler et al. 2014). As discomfort and awareness were not assessed in the animals in the current study, we use the term hyperacusis to describe hyper-responsiveness during ASR testing. Other studies have reported hyperacusis in both salicylate (Holt et al. 2010; Sun et al. 2009; Turner et al. 2006) and noise-exposed animals (Hickox and Liberman 2014; Knipper et al. 2013; Turner et al. 2006, 2012; Turner and Larsen 2016; Salloum et al. 2014). Peripheral synaptopathy (loss of inner hair cell synapses) has been speculated to be a potential root cause in studies where noise trauma results in a return to normal hearing thresholds (2–7 days), but with residual hyperacusis during the first few weeks (Hickox and Liberman 2014; Kujawa and Liberman 2009). One measure of this synaptopathy has been evaluation of wave I ABR amplitude. In the current study, in the TTS group, when hearing thresholds had returned to normal, mid-high frequencies showed supra-normal amplitudes after 2 months. Could this increase in responsiveness result in hyperacusis and/or tinnitus? Can hyperacusis be an indicator of tinnitus. Some have hypothesized that synaptopathy-related hyperacusis may be due to overcompensation in the central nervous system (Knipper et al. 2013). The timing of hyperacusis after cochlear trauma may represent crucial periods for peripheral and central dynamic plastic changes. Hyperacusis was observed at specific frequencies, suggesting that hyperacusis may be frequency specific and not necessarily in the same frequency range as the noise exposure or hearing deficits (Auerbach et al. 2014; Turner and Larsen 2016).

Previously, our work and others have reported results from ASR testing following noise exposure (Hickox and Liberman 2014; Holt et al. 2010; Turner and Parrish 2008). However, our current results fit well with recent studies indicating that changes in GAP detection status continue to occur over time and thus expanding the incidence of ASR testing is prudent (Turner and Larsen 2016). Frequent testing can reduce total startle to such an extent that no differences in startle can be discerned in the presence or absence of the gap of silence. However, infrequent testing may not capture the extent or the nature of changes occurring in detection of the silent gap after acoustic trauma, giving the impression that GAP detection irregularities are episodic. Therefore, reporting data from individual testing sessions may also prove instructive (Altschuler et al. 2015).

The two noise exposure paradigms that we employed represent two tinnitus models that have been well characterized. The mild noise exposure TTS model is from the Bauer and Brozoski group while the severe noise exposure PTS model is from the Kaltenbach group. Both models have shown behavioral evidence of tinnitus (Brozoski et al. 2007; Heffner and Harrington 2002; Turner et al. 2006) and changes in neuronal activity. The basis for using these models is that commonalities observed between the two groups are more likely due to tinnitus than to hearing loss only (PTS) or acoustic trauma only (TTS), while differences are likely due to either the specific nature of PTS or TTS. At the frequencies we used for the noise exposure, the SD male Sprague Dawley rat model results in tinnitus following acoustic trauma in nearly 100% of the animals (Heffner 2011). Therefore, our results suggest that GAP detection irregularities, whether deficits or enhancements, may be indicators of tinnitus. Since inhibition of ASR involves several brain regions, differences in GAP detection suggest involvement of central neuronal pathways.

In addition to GAP detection irregularities, multiple studies have linked loud noise exposure with increased SNA in auditory pathways (Auerbach et al. 2014; Holt et al. 2010; Mulders et al. 2011; Mulders and Robertson 2011, 2013; Robertson et al. 2013). Specifically, the two noise exposures (PTS—Heffner and Harrington 2002; Zhang and Kaltenbach 1998; TTS—Brozoski et al. 2007) used in the current study have been reported to result in tinnitus and increased SNA. Increased SNA has been touted as the primary indicator of tinnitus. One concern with this indicator is that noise-related increases in SNA are often delayed by hours or days even when psychophysical data report an immediate onset for noise-induced tinnitus (Heffner and Harrington 2002). Interestingly, there have been reports of changes in SNA immediately after noise exposure. Initially, after exposure to loud noise producing hearing loss, neurons of the DCN display decreased SNA (Kaltenbach et al. 2000). Decreased SNA has also been reported in the IC days and months after noise exposure (Basta and Ernest 2004; Chen et al. 2016; Gerken et al. 1984; Ropp et al. 2014). Two months after noise exposure, reduced spontaneous firing is reported in specific IC neurons in animals with behavioral evidence of tinnitus (Ropp et al. 2014). A relationship has been shown between the intensity of a noise exposure and changes in the localization and direction of SNA. Focal regions of reduced glucose uptake, used as a measure of SNA in the IC (Jones and Disterhoft 1983), are observed in the CNIC 2 months after broad band noise exposure. They reported that at 100 dB SPL there was a significant increase in SNA in the CNIC. However, 110 dB SPL and 120 dB SPL noise exposures resulted in growing regions of substantially reduced glucose levels located centrally, surrounded by regions of increased glucose uptake (Ryan et al. 1992). This is similar to the current study in which exposures of 106 dB SPL (TTS) and 118 dB SPL 1/3 octave band were used to generate tinnitus. These data along with other studies suggest that tinnitus can be associated with neuronal *hypoactivity* (Luo et al. 2014; Yang et al. 2007).

MEMRI can be used to probe neuronal activity in both PTS and TTS models in–vivo—Manganese, administered to the awake and freely moving rat, is taken into cells primarily via L-type calcium channels with slow manganese efflux from the cell (days to weeks). Thus, manganese encodes the history of L-type calcium channel function while the animal is awake and freely moving (Cacace et al. 2014). Specifically, in the auditory system MEMRI has been validated as a marker of neuronal activity (reviewed in Cacace et al. 2014). Initial studies using MEMRI to evaluate the auditory system demonstrated that louder noise resulted in more Mn^{2+} uptake in the IC. When animals administered Mn^{2+} were exposed to high and low frequency tones, increased contrast was observed in corresponding tonotopic regions of the IC (Yu et al. 2011, 2005, 2008). This MEMRI index of neuronal activity has been used previously to examine tinnitus-related changes *ex-vivo* (Brozoski et al. 2007, 2013). Using MEMRI to examine neuronal activity after death has limitations because ultimately this approach does not allow assessment of neuronal activity over time. Because our ASR results demonstrated time dependent changes, inability to examine SNA over time may result in critical time points in acoustic-trauma-related changes being overlooked. In addition, Mn^{2+} levels and/ or MRI T1 signals may change after death. Here, we use MEMRI to examine neuronal changes in live animals, preserving the potential for studying SNA in animals longitudinally. In the current study, Mn^{2+} uptake was evaluated using signal intensity from T_1-weighted images with muscle used to normalize each brain

region. Muscle normalization was performed to control for minor variations in Mn^{2+} administration that may result in differences in the amount of Mn^{2+} available for uptake in each animal and coil performance during a given MRI session. Previous studies have examined changes in neuronal activity using electrophysiology up to two weeks following a PTS noise exposure in guinea pigs (Mulders and Robertson 2013) and MEMRI 48 h following a PTS noise exposure in rats (Holt et al. 2010) with behavioral evidence of tinnitus. We compared the TTS group and the PTS group to controls 2 months following noise exposure. In the PTS group the DCN, DCIC, and AC had significant decreases in Mn^{2+} uptake, suggesting significant decreases in neuronal activity. Noise-induced changes in neuronal activity have been postulated to result initially from habituation to the noise exposure and then from lateral inhibition during attempts at homeostatic rebalancing of auditory pathways over time after noise exposure (Pienkowski and Eggermont 2012; Turrigiano 1999, 2011; Turrigiano and Nelson 2004).

Several studies have previously demonstrated increases in Mn^{2+} uptake after behavioral evidence of tinnitus. The decrease in noise-induced Mn^{2+} uptake at 2 months may be the result of a decrease in cell size, a decrease in the number of neurons, perhaps reflecting chronic energy reduction as the cells undergo oxidative stress, or a loss or change in the number and/or types of voltage gated calcium channels expressed by neurons. Another idea is that the effects of peripheral synaptopathy, a loss of inner hair cell synapses, is propagated throughout the auditory pathway over time. To address this question, future studies will need to assess inner hair cell synaptic markers to evaluate synaptic loss in addition to comparing the amplitude of ABR waveforms specific to peripheral or central function.

There were also changes in the pattern of manganese uptake in auditory pathways (Fig. 11) after both PTS and TTS. Both in the PTS and TTS groups there was a shift from the highest level of manganese uptake from the DCN to the SOC and PVCN. To better understand the relationship between Mn^{2+} uptake, tinnitus and/or hearing loss, changes in Mn^{2+} uptake will need to be studied longitudinally following a noise exposure and correlated with GAP detection performance.

Using MEMRI as a tool for tonotopic analysis—The noninvasive nature of MEMRI makes it a useful tool to assess tonotopic organization within key auditory brain regions, previously studied using electrophysiology (Hackett et al. 2011; Romand and Ehret 1990) and in a more limited way using MEMRI (Yu et al. 2007). When examining regional differences in the distribution of M n^{2+} within the CNIC, we found significantly lower Mn^{2+} uptake in the ventral region of the CNIC of the PTS group compared to controls. In the Sprague Dawley rat, ventromedial regions of the CNIC correspond to high frequency while dorsolateral regions correlate with low frequency (Huang and Fex 1986). Our data are similar to those of studies where metabolic activity was measured following intense noise exposure (Ryan et al. 1992). In these studies, wide band noise (1.414–5.656 kHz) produced different patterns of metabolic activity in the CN and CNIC depending upon the level of the exposure. The 100 dB SPL produced broad spread increases in metabolic activity, while the 110 and 120 dB SPL exposures left the most dorsal and ventral regions with high activity, and a central (mid dorsal) to ventral region with greatly diminished activity. In our study, a 1/3 octave 118 dB SPL exposure also left a central–ventral region pattern of significantly

diminished Mn^{2+} uptake. This implicates changes in the activity of mid to high frequency neurons in the CNIC. Our results complement other studies that demonstrate that loud noise affects low spontaneous firing rate, high threshold auditory nerve fibers. In the IC high frequency neurons are the most affected following acoustic trauma (Bures et al. 2010; Grécová et al. 2009) suggesting that auditory nerve fiber trauma may be propagated centrally. Since MEMRI is highly sensitive to changes in neuronal activity and has high spatial resolution (Cacace et al. 2014) this technique will be helpful in future examination of tonotopic changes in auditory nuclei over time as synaptopathy, hearing loss, and/or tinnitus progresses.

Overall, querying the relative Mn^{2+} uptake of auditory brain regions may begin to provide a map of activity levels following acoustic trauma and provide clues about pathway activity reorganization and their relationship to changes in hearing sensitivity and tinnitus. Two months following acoustic trauma, some changes in Mn^{2+} uptake within the auditory pathway are similar. The SOC becomes the most active region followed by the PVCN in both the TTS and the PTS groups (Fig. 11). Since these changes occur in both groups they are independent of hearing status. This is in contrast to the IC where there are differential changes in Mn^{2+} uptake, with the DCIC taking up the highest level of Mn^{2+} in the TTS group and taking up the least in the PTS groups compared to the other two IC subdivisions. These differences in Mn^{2+} in the IC suggest that MEMRI can discriminate hearing specific differences centrally following acoustic trauma. Whether features such as severity of damage, frequency at which damage occurs, etc.. can be identified using this method remain to be tested. Cochlear nucleus inputs to IC neurons are excitatory while SOC inputs are both inhibitory and excitatory. Thus reduced input from CN and increased input from SOC could contribute to increased inhibition of IC neurons. In addition, changes in the level of inhibitory neurotransmitter in the IC can change inhibitory tone in the nucleus. Changes in IC inhibition, which has been reported to occur following acoustic trauma (Turner et al. 2013), could result in decreased Mn^{2+} uptake. In the future, correlating synapse loss in the periphery, with neurotransmitter levels, SNA, and Mn^{2+} uptake centrally may prove useful.

Correlating GAP detection and MEMRI to distinguish tinnitus and hyperacusis —By correlating Mn^{2+} uptake with GAP detection we may also learn whether ASR and MEMRI can be used together as an objective measure of tinnitus regardless of hearing status. In the current study, the correlation of frequency specific GAP detection to MEMRI in the DCN and DCIC revealed a significant negative correlation for the TTS group. At 12 kHz in the control group, the amount of Mn^{2+} uptake was higher in those animals with better GAP detection both at baseline and 5–8 weeks later. In the TTS group the same pattern was observed at baseline, higher Mn^{2+} uptake in better ASR performing animals at 12 kHz. However, at 5–8 weeks after noise exposure, higher Mn^{2+} uptake was correlated with poorer GAP detection. This fits well with the hypotheses that (1) normal hearing would result in a positive correlation (Fig. 12 control) between Mn^{2+} uptake and GAP detection i.e., better GAP detection with more Mn^{2+} uptake; (2) tinnitus would result in an inverse correlation (Fig. 12 tinnitus) with more Mn^{2+} uptake (increased SNA) and more GAP detection deficits; (3) that hearing deficits would result in a positive correlation i.e., poor GAP detection with poor Mn^{2+} uptake (Fig. 12 Hearing Loss); and (4) hyperacusis with tinnitus would result in

enhanced GAP detection and good Mn^{2+} uptake, while hyperacusis with hearing loss would result in GAP detection deficits and poor Mn^{2+} uptake. In this proposed correlation, GAP detection irregularities (decreased or increased ability to detect the silent gap) during ASR testing can be correlated with tinnitus. This model stresses the need to determine brain regions, frequencies, and time points that can reliably be applied. Further testing of this correlation would be useful in a longitudinal study where data from multiple ASRs and imaging sessions would be collected before and several times after noise exposure in the same animals.

Conclusions

Changes in the pattern of Mn^{2+} uptake are evident at 2 months after noise exposure and suggest that these changes within the auditory pathway may reflect adjustments to central gain necessary to maintain synaptic and intrinsic homeostasis. Interestingly, noise exposure results in a pattern of Mn^{2+} uptake that when combined with GAP detection, may allow discrimination of hearing loss from tinnitus. These data raise the question of whether observed differences are static or continue to change over time. Our previous data using MEMRI in vivo demonstrated that noise-induced PTS results in increased Mn^{2+} uptake 48 h after induction. However, in the current study, after 2 months the level of Mn^{2+} uptake is less than that observed in normal hearing animals. Therefore, long-term hearing threshold elevation can result in diminished neuronal activity in the brainstem, midbrain, and cortex that change over time. This hypoactivity, relative to normal hearing controls, combined with either reduced GAP detection, increased sensitivity to sound as measured by enhanced GAP detection and increased ABR wave 1 amplitude may each be consistent with the tinnitus experience.

In addition to using MEMRI as a proxy for examining spontaneous neuronal activity associated with tinnitus, as in the present study, Mn^{2+} uptake could also be studied in response to noise stimulation following the onset of tinnitus. This is especially relevant given a recent study demonstrating a subpopulation of neurons in the IC that produce a long lasting after discharge in response to sound that can last for minutes after the sound has stopped (Ono et al. 2016). Tinnitus may reflect an inability of these IC neurons to produce the after discharge. Thus MEMRI may reflect this change in afferent activity as decreased Mn^{2+} uptake. Future MEMRI studies could examine sound driven Mn^{2+} uptake in tinnitus models to determine whether after discharges in the IC are reduced, the time point at which the loss of after discharges occur, and how long this change is maintained after the onset of tinnitus.

Although, noise generated enhancement of GAP detection and MRI detectable *depression* of neuronal activity in auditory-related brain regions may challenge current accepted notions of tinnitus measures, these features should also be considered as indicators of tinnitus. Having the ability to assess and monitor the activity of neurons within the auditory pathway greatly enhances the understanding of hearing-related pathology and the probability of devising effective treatment for hearing loss and tinnitus. Our results support the use of MEMRI, ABR, and ASR as useful and sensitive tools to evaluate changes in central gain, inhibition, and neuronal activity whether generated following mild or severe acoustic trauma. The

results also continue to build a case for combining the use of MEMRI and inhibition of ASR as objective measures of tinnitus.

Acknowledgements

We thank Mohanned Ahmed, Ahmad Ali Nassar, Sharowynn Wilson, and Nour Arafat for their help with experiments, analysis and creating macros for data analysis. A special thank you to Drs. P. D. Walker and R. Braun for providing feedback on the article prior to submission.

Funding This work was supported by the Department of Veterans Affairs (Grant 1I01RX001095–01U.S to A.G.H); the National Institute for Occupational Safety and Health, Centers for Disease Control and Prevention (training Grant T42 OH008455 to AGH and AKA); the National Institutes of Health (Grant EY021619 to BAB); and Research to Prevent Blindness (unrestricted Grant to BAB). The views expressed do not necessarily reflect the official policies of the Department of Health and Human Services, nor does mention of trade names, commercial practices, or organizations imply endorsement by the US Government.

References

Altschuler RA, Dolan DF, Halsey K, Kanicki A, Deng N, Martin C, Eberle J, Kohrman DC, Miller RA, Schacht J (2015) Age-related changes in auditory nerve-inner hair cell connections, hair cell numbers, auditory brain stem response and gap detection in UMHET4 mice. Neuroscience 292:22–33 [PubMed: 25665752]

Auerbach BD, Rodrigues PV, Salvi RJ (2014) Central gain control in tinnitus and hyperacusis. Front Neurol 5:206 [PubMed: 25386157]

Baizer JS, Manohar S, Paolone NA, Weinstock N, Salvi RJ (2012) Understanding tinnitus: The dorsal cochlear nucleus, organization and plasticity. Brain Res 1485:40–53 [PubMed: 22513100]

Basta D, Ernest A (2004) Noise-induced changes of neuronal spontaneous activity in mice inferior colliculus brain slices. Neurosci Lett 368(3):297–302 [PubMed: 15364415]

Bissig D, Berkowitz BA (2014) Testing the calcium hypothesis of aging in the rat hippocampus in vivo using manganese-enhanced MRI. Neurobiol Aging 35(6):1453–1458 [PubMed: 24439958]

Brozoski TJ, Bauer CA, Caspary DM (2002) Elevated fusiform cell activity in the dorsal cochlear nucleus of chinchillas with psychophysical evidence of tinnitus. J Neurosci 22(6):2383–2390 [PubMed: 11896177]

Brozoski TJ, Ciobanu L, Bauer CA (2007) Central neural activity in rats with tinnitus evaluated with manganese-enhanced magnetic resonance imaging (MEMRI). Hear Res 228(1–2):168–179 [PubMed: 17382501]

Brozoski TJ et al. (2010) The effect of supplemental dietary taurine on tinnitus and auditory discrimination in an animal model. Hear Res 270(1–2):71–80 [PubMed: 20868734]

Brozoski TJ, Wisner KW, Odintsov B, Bauer CA (2013) Local NMDA receptor blockade attenuates chronic tinnitus and associated brain activity in an animal model. Plos One 8(10):e77674 [PubMed: 24282480]

Bures Z, Grécová J, Popelár J, Syka J (2010) Noise exposure during early development impairs the processing of sound intensity in adult rats. Eur J Neurosci 32:155–164 [PubMed: 20597969]

Cacace AT, Brozoski T, Berkowitz B, Bauer C, Odintsov B, Bergkvist M, Castracane J, Zhang J, Holt AG (2014) Manganese enhanced magnetic resonance imaging (MEMRI): a powerful new imaging method to study tinnitus. Hear Res 311:49–62 [PubMed: 24583078]

Carlson S, Willott JF (1996) The behavioral salience of tones as indicated by prepulse inhibition of the startle response: relationship to hearing loss and central neural plasticity in C57BL/6J mice. Hear Res 99(1–2):168–175 [PubMed: 8970825]

Campolo J, Lobarinas E, Salvi R (2013) Does tinnitus “fill in” the silent gaps? Noise Health 15(67): 398–405 [PubMed: 24231418]

Chen GD, Sheppard A, Salvi R (2016) Noise trauma induced plastic changes in brain regions outside the classical auditory pathway. Neuroscience 315:228–245 [PubMed: 26701290]

Chuang KH, Koretsky AP, Sotak CH (2009) Temporal changes in the T1 and T2 relaxation rates (DeltaR1 and DeltaR2) in the rat brain are consistent with the tissue-clearance rates of elemental manganese. Magn Reson Med 61(6):1528–1532 [PubMed: 19353652]

Davis (1984) The mammalian startle response In: Eaton RC (ed) Neural mechanisms of startle behavior Plenum Press, New York, pp 287–351

Eggermont JJ, Roberts LE (2004) The neuroscience of tinnitus. Trends Neurosci 27(11):676–682 [PubMed: 15474168]

Galazyuk A, Hébert S (2015) Gap-prepulse inhibition of the acoustic startle reflex (GPIAS) for tinnitus assessment: current status and future directions. Front Neurol 6:88 [PubMed: 25972836]

Gerken GM, Saunders SS, Paul RE (1984) Hypersensitivity to electrical stimulation of auditory nuclei follows hearing loss in cats. Hear Res 13(3):249–259 [PubMed: 6735932]

Grécová J, Bures Z, Popelár J, Suta D, Syka J (2009) Brief exposure of juvenile rats to noise impairs the development of the response properties of inferior colliculus neurons. Eur J Neurosci 29:1921–1930 [PubMed: 19473244]

Hackett TA, Barkat TR, O'Brien BM, Hensch TK, Polley DB (2011) Linking topography to tonotopy in the mouse auditory thalamocortical circuit. J Neurosci 31(8):2983–2995 [PubMed: 21414920]

Heffner HE (2011) A two-choice sound localization procedure for detecting lateralized tinnitus in animals. Behav Res Methods 43(2):577–589 [PubMed: 21416307]

Heffner HE, Harrington IA (2002) Tinnitus in hamsters following exposure to intense sound. Hear Res 170(1–2):83–95 [PubMed: 12208543]

Hickox AE, Liberman MC (2014) Is noise-induced cochlear neuropathy key to the generation of hyperacusis or tinnitus? J Neurophysiol 111

Holt AG, Bissig D, Mirza N, Rajah G, Berkowitz B (2010) Evidence of key tinnitus-related brain regions documented by a unique combination of manganese-enhanced MRI and acoustic startle reflex testing. Plos One 5(12):e14260 [PubMed: 21179508]

Huang CM, Fex J (1986) Tonotopic organization in the inferior colliculus of the rat demonstrated with the 2-deoxyglucose method. Exp Brain Res 61(3):506–512 [PubMed: 3956611]

Ison JR, Allen PD (2003) Low-frequency tone pips elicit exaggerated startle reflexes in C57BL/6J mice with hearing loss. J Assoc Res Otolaryngol 4(4):495–504 [PubMed: 12784135]

Jastreboff PJ, Hazell JWP (1993) A neurophysiological approach to tinnitus—clinical implications. Br J Audiol 27(1):7–17 [PubMed: 8339063]

Jones LS, Disterhoft JF (1983) The effect of auditory stimulus rate on [14C]2-deoxyglucose uptake in rabbit inferior colliculus. Brain Res 279(1–2):85–91 [PubMed: 6640357]

Kaltenbach JA, Zhang J, Afman CE (2000) Plasticity of spontaneous neural activity in the dorsal cochlear nucleus after intense sound exposure. Hear Res 147(1–2):282–292 [PubMed: 10962192]

Kaltenbach JA, Zhang J, Finlayson P (2005) Tinnitus as a plastic phenomenon and its possible neural underpinnings in the dorsal cochlear nucleus. Hear Res 206(1–2):200–226 [PubMed: 16081009]

Knipper M, Van Dijk P, Nunes I, Ruttiger L, Zimmermann U (2013) Advances in the neurobiology of hearing disorders: recent developments regarding the basis of tinnitus and hyperacusis. Prog Neurobiol 111:17–33 [PubMed: 24012803]

Koch (1999) The neurobiology of startle. Prog Neurobiol 59:107–128 [PubMed: 10463792]

Kujawa SG, Liberman MC (2009) Adding insult to injury: cochlear nerve degeneration after "temporary" noise-induced hearing loss. J Neurosci 29(45):14077–14085 [PubMed: 19906956]

Lobarinas E, Salvi R, Baizer J, Altman C, Allman B (2013) Noise and health special issue: advances in the neuroscience of tinnitus. Noise Health 15(63):81–82 [PubMed: 23571296]

Lockwood AH, Salvi RJ, Coad ML, Towsley ML, Wack DS, Murphy BW (1998) The functional neuroanatomy of tinnitus—evidence for limbic system links and neural plasticity. Neurology 50(1):114–120 [PubMed: 9443467]

Longenecker RJ, Galazyuk AV (2011) Development of tinnitus in CBA/CaJ mice following sound exposure. J Assoc Res Otolaryngol 12(5):647–658 [PubMed: 21667173]

Longenecker RJ, Galazyuk AV (2012) Methodological optimization of tinnitus assessment using prepulse inhibition of the acoustic startle reflex. Brain Res 1485:54–62 [PubMed: 22513102]

Longenecker RJ, Chonko KT, Maricich SM, Galazyuk AV (2014) Age effects on tinnitus and hearing loss in CBA/CaJ mice following sound exposure. SpringerPlus 3(1):1–13 [PubMed: 24422185]

Luo H, Pace E, Zhang X, Zhang J (2014) Blast-Induced tinnitus and spontaneous firing changes in the rat dorsal cochlear nucleus. J Neurosci Res 92(11):1466–1477 [PubMed: 24938852]

McCormack A, Edmondson-Jones M, Somerset S, Hall D (2016) A systematic review of the reporting of tinnitus prevalence and severity. Hear Res 337:70–79 [PubMed: 27246985]

Mulders WHAM, Robertson D (2011) Progressive centralization of midbrain hyperactivity after acoustic trauma. Neuroscience 192:753–760 [PubMed: 21723924]

Mulders WHAM, Robertson D (2013) Development of hyperactivity after acoustic trauma in the guinea pig inferior colliculus. Hear Res 298:104–108 [PubMed: 23276730]

Mulders WH, Ding D, Salvi R, Robertson D (2011) Relationship between auditory thresholds, central spontaneous activity, and hair cell loss after acoustic trauma. J Comp Neurol 519(13):2637–2647 [PubMed: 21491427]

Ono M, Bishop DC, Oliver DL (2016) Long-lasting sound-evoked afterdischarge in the auditory midbrain. Sci Rep 6:20757 [PubMed: 26867811]

Paxinos G, Watson C (2007) The rat brain in stereotaxic coordinates. Elsevier, Amsterdam

Pienkowski M, Eggermont JJ (2012) Reversible long-term changes in auditory processing in mature auditory cortex in the absence of hearing loss induced by passive, moderate-level sound exposure. Ear Hear 33:305–314 [PubMed: 22343545]

Robertson D, Bester C, Vogler D, Mulders WHAM. (2013) Spontaneous hyperactivity in the auditory midbrain: Relationship to afferent input. Hear Res 295:124–129 [PubMed: 22349094]

Romand R, Ehret G (1990) Development of tonotopy in the inferior colliculus. I. Electrophysiological mapping in house mice. Brain Res Dev Brain Res 54(2):221–234 [PubMed: 2397588]

Ropp TJ, Tiedemann KL, Young ED, May BJ (2014) Effects of unilateral acoustic trauma on tinnitus-related spontaneous activity in the inferior colliculus. J Assoc Res Otolaryngol JARO 15(6):1007–1022 [PubMed: 25255865]

Rorden C, Brett M (2000) Stereotaxic display of brain lesions. Behav Neurol 12(4):191–200 [PubMed: 11568431]

Ryan AF, Axelsson GA, Woolf NK (1992) Central auditory metabolic activity induced by intense noise exposure. Hear Res 61(1–2):24–30 [PubMed: 1326506]

Rybalko N, Bureš Z, Burianová J, Popelář J, Grécová J, Syka J (2011) Noise exposure during early development influences the acoustic startle reflex in adult rats. Physiol Behav 102:453–458 [PubMed: 21192960]

Salvi RJ, Arehole S (1985) Gap detection in chinchillas with temporary high-frequency hearing-loss. J Acoust Soc Am 77(3):1173–1177 [PubMed: 3980869]

Salloum RH, Yurosko C, Santiago L, Sandridge SA, Kaltenbach JA (2014) Induction of enhanced acoustic startle response by noise exposure: dependence on exposure conditions and testing parameters and possible relevance to hyperacusis. PLoS One 9(10):e111747 [PubMed: 25360877]

Shargorodsky J, Curhan GC, Farwell WR (2010) Prevalence and characteristics of tinnitus among US adults. Am J Med 123

Shore S, Zhou JX, Koehler S (2007) Neural mechanisms underlying somatic tinnitus. Prog Brain Res 166:107–123 [PubMed: 17956776]

Silva AC, Bock NA (2008) Manganese-enhanced MRI: an exceptional tool in translational neuroimaging. Schizophr Bull 34(4):595–604 [PubMed: 18550591]

Sun W, Lu J, Stolzberg D, Gray L, Deng A, Lobarinas E, Salvi RJ (2009) Salicylate increases the gain of the central auditory system. Neuroscience 159(1):325–334 [PubMed: 19154777]

Swerdlow N et al. (2001) Neural circuit regulation of prepulse inhibition of startle in the rat: current knowledge and future challenges. Psychopharmacology (Berl) 156(2–3):194–215 [PubMed: 11549223]

Takeda A (2003) Manganese action in brain function. Brain Res Rev 41(1):79–87 [PubMed: 12505649]

Turner JG, Larsen D (2016) Effects of noise exposure on development of tinnitus and hyperacusis: prevalence rates 12 months after exposure in middle-aged rats. Hear Res 334:30–36 [PubMed: 26584761]

Turner JG, Parrish J (2008) Gap detection methods for assessing salicylate-induced tinnitus and hyperacusis in rats. Am J Audiol 17(2):S185–S192 [PubMed: 18978200]

Turner JG, Brozoski TJ, Bauer CA, Parrish JL, Myers K (2006) Gap detection deficits in rats with tinnitus: a potential novel screening tool. Behav Neurosci 120(1):188–195 [PubMed: 16492129]

Turner J, Larsen D, Hughes L, Moechars D, Shore S (2012) Time course of tinnitus development following noise exposure in mice. J Neurosci Res 90(7):1480–1488 [PubMed: 22434653]

Turner JG, Parrish JL, Zuiderveld L, Darr S, Hughes LF, Caspary DM, Idrezbegovic E, Canlon B (2013) Acoustic experience alters the aged auditory system. Ear Hear 34:151–159 [PubMed: 23086424]

Turrigiano GG (1999) Homeostatic plasticity in neuronal networks: the more things change, the more they stay the same. Trends Neurosci 22:221–227 [PubMed: 10322495]

Turrigiano G (2011) Too many cooks? Intrinsic and synaptic homeostatic mechanisms in cortical circuit refinement. Annu Rev Neurosci 34:89–103 [PubMed: 21438687]

Turrigiano GG, Nelson SB (2004) Homeostatic plasticity in the developing nervous system. Nat Rev Neurosci 5:97–107 [PubMed: 14735113]

Tyler RS, Pienkowski M, Roncancio ER, Jun HJ, Brozoski T, Dauman N, Coelho CB, Andersson G, Keiner AJ, Cacace AT (2014) A review of hyperacusis and future directions: part I. Definitions and manifestations. Am J Audiol 23(4):402–419 [PubMed: 25104073]

Van de Moortele PF, Auerbach EJ, Olman C, Yacoub E, Ugurbil K, Moeller S (2009) T1 weighted brain images at 7 T unbiased for Proton Density, T2* contrast and RF coil receive B1 sensitivity with simultaneous vessel visualization. Neuroimage 46(2):432–446 [PubMed: 19233292]

Yang G, Lobarinas E, Zhang L, Turner J, Stolzberg D, Salvi R, Sun W (2007) Salicylate induced tinnitus: behavioral measures and neural activity in auditory cortex of rats. Hear Res 226(1–2): 244–253 [PubMed: 16904853]

Young JS, Fechter LD (1983) Reflex inhibition procedures for animal audiometry: a technique for assessing ototoxicity. J Acoust Soc Am 73(5):1686–1693 [PubMed: 6615589]

Yu X, Wadghiri YZ, Sanes DH, Turnbull DH (2005) In vivo auditory brain mapping in mice with Mn-enhanced MRI. Nat Neurosci 8(7):961–968 [PubMed: 15924136]

Yu X, Sanes DH, Aristizabal O, Wadghiri YZ, Turnbull DH (2007) Large-scale reorganization of the tonotopic map in mouse auditory midbrain revealed by MRI. Proc Natl Acad Sci USA 104(29): 12193–12198 [PubMed: 17620614]

Yu X, Zou J, Babb JS, Johnson G, Sanes DH, Turnbull DH (2008) Statistical mapping of sound-evoked activity in the mouse auditory midbrain using Mn-enhanced MRI. NeuroImage 39(1):223–230 [PubMed: 17919926]

Yu X, Nieman BJ, Sudarov A, Szulc KU, Abdollahian DJ, Bhatia N, Lalwani AK, Joyner AL, Turnbull DH (2011) Morphological and functional midbrain phenotypes in Fibroblast Growth Factor 17 mutant mice detected by Mn-enhanced MRI. Neuroimage 56(3):1251–1258 [PubMed: 21356319]

Zhang JS, Kaltenbach JA (1998) Increases in spontaneous activity in the dorsal cochlear nucleus of the rat following exposure to highintensity sound. Neurosci Lett 250(3):197–200 [PubMed: 9708866]

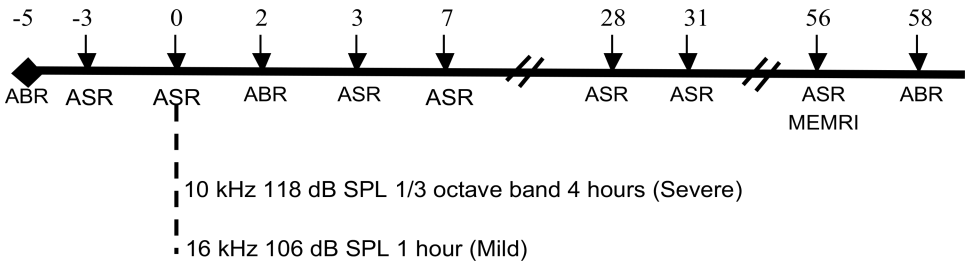

Fig. 1.

A timeline depicting when behavioral, hearing and MEMRI testing occurred. The numbers represent the day that testing took place relative to a severe or mild noise exposure (dashed vertical line). Parallel angled lines represent ASR testing (2–3 times per week) from days 8–28 and days 34–56. *ABR* auditory brainstem response, *ASR* acoustic startle reflex, *MEMRI* manganese enhanced MRI

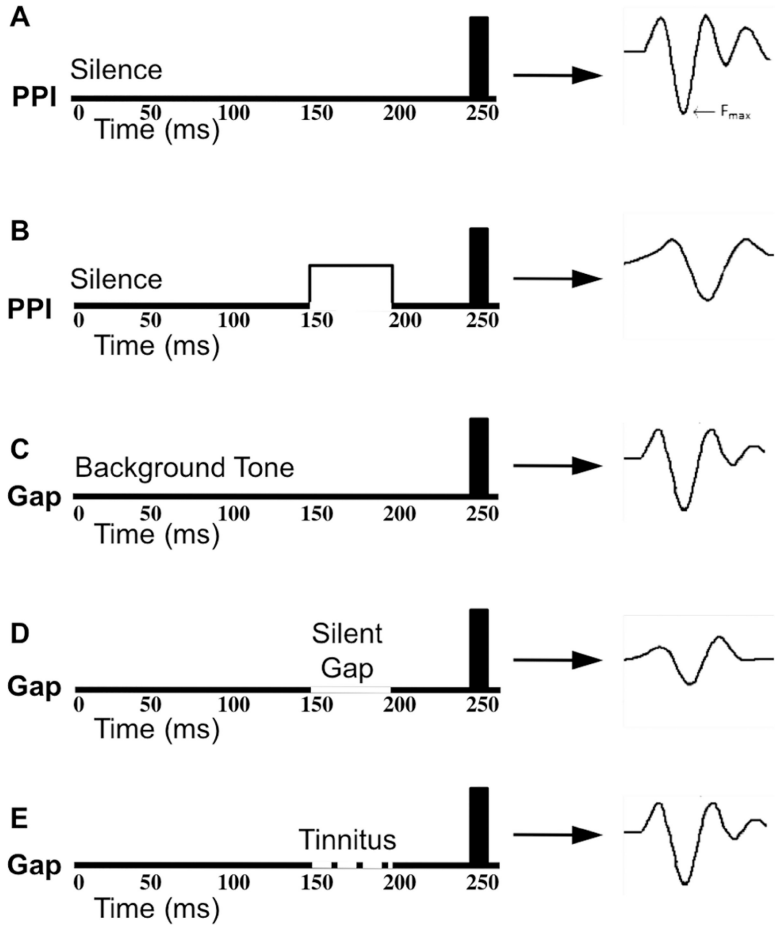

Fig. 2.

Pre-pulse inhibition and GAP detection to determine hearing sensitivity (**a, b**) and tinnitus status (**c**–**e**). For pre-pulse inhibition, a maximum startle response is established by interjecting a startle noise (20 ms, 120 dB SPL broadband noise) during a silent interlude (**a**). To measure inhibition of this startle response, a period of silence is interrupted by a 50 ms tone 50 ms prior to the 20 ms startle noise (**b**). For GAP inhibition testing, the maximum startle responses with and without the background tone are determined (**c**). During GAP testing, a continuous carrier tone is interrupted by a 50 ms silent period (GAP) 50 ms prior to a 120 dB startle sound (**d**). If an animal experiences tinnitus at a frequency similar to that of the carrier tone then the tinnitus will interfere with GAP detection and the reduction in startle response will not be blunted (**e**)

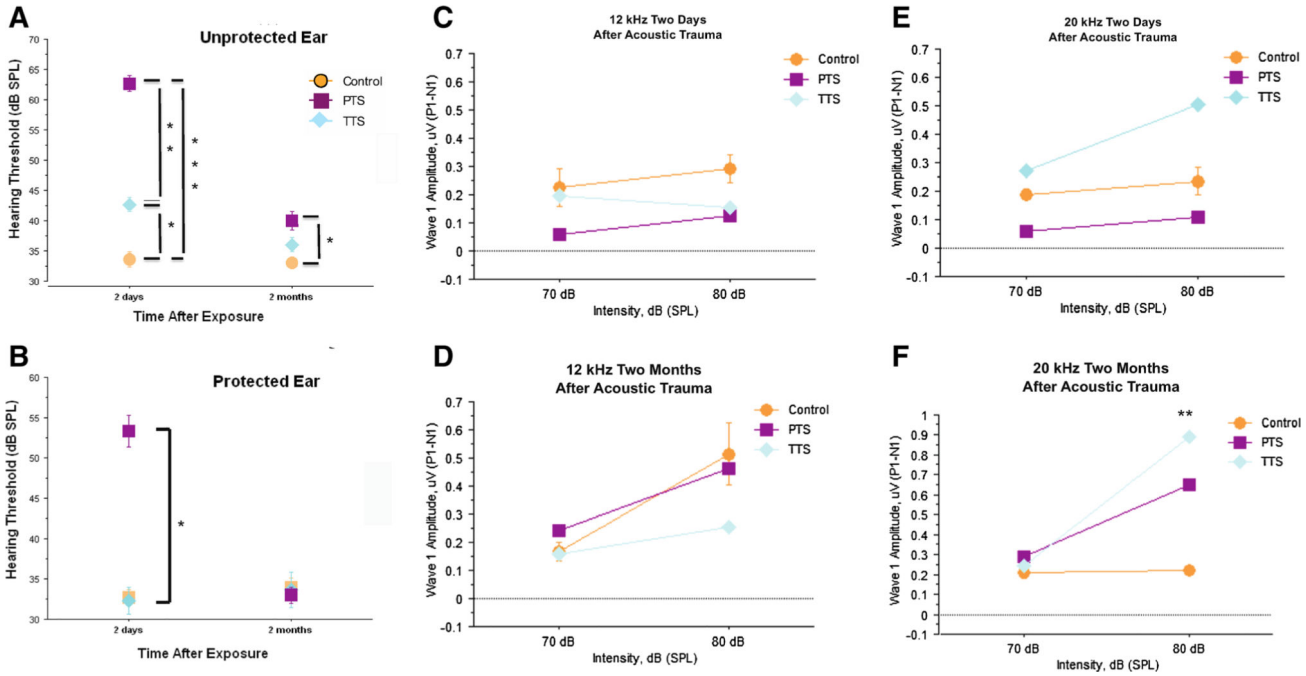

Fig. 3.

Mild and severe noise exposures result in a temporary threshold shift (TTS) and a permanent threshold shift (PTS) as well as alterations in wave I amplitude after 2 months. Animals sustaining a TTS had thresholds different from the control group (**a**). Threshold shifts in the unprotected, and protected ear were compared 2 days and 2 months after noise exposure (**a, b**). Wave I amplitude (μV) was measured across 70–80 dB SPL at 12 kHz (**c**) and 20 kHz (**e**) 2 days following noise exposure when compared to controls. Wave I amplitude was also measured 2 months after the acoustic trauma at the same frequencies, 12 kHz (**d**) and 20 kHz (**f**). **p* value ≤ 0.05, ***p* value of 0.01–0.05; ****p* value of 0.001–0.005

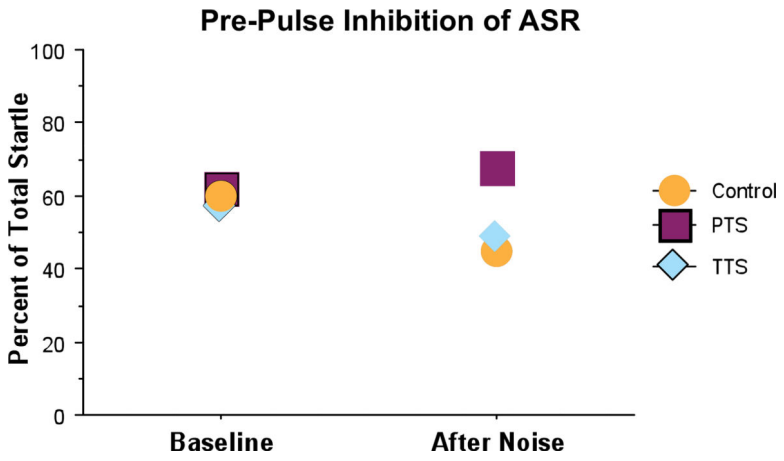

Fig. 4.

Pre-pulse inhibition of ASR before and after exposure to a noise (PTS 10 kHz 118 dB 1/3 octave band, 4 h; TTS 16 kHz 106 dB, 1 h) compared to controls (no noise exposure). Subjects displayed reduced startle responses during pre-pulse testing both before and after exposure to noise

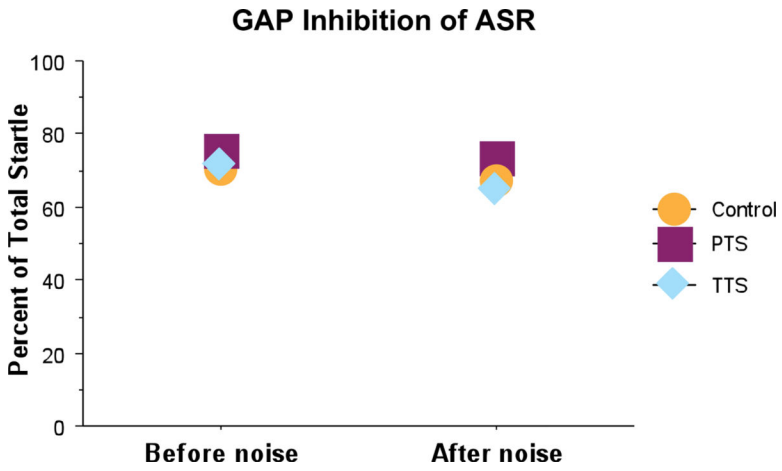

Fig. 5.

GAP detection before and after exposure to noise (PTS 10 kHz 118 dB 1/3 octave band, 4 h; TTS 16 kHz 106 dB, 1 h) compared to controls (no noise exposure). Generally, subjects demonstrated reduced startle responses during GAP detection testing, both before and after exposure to noise

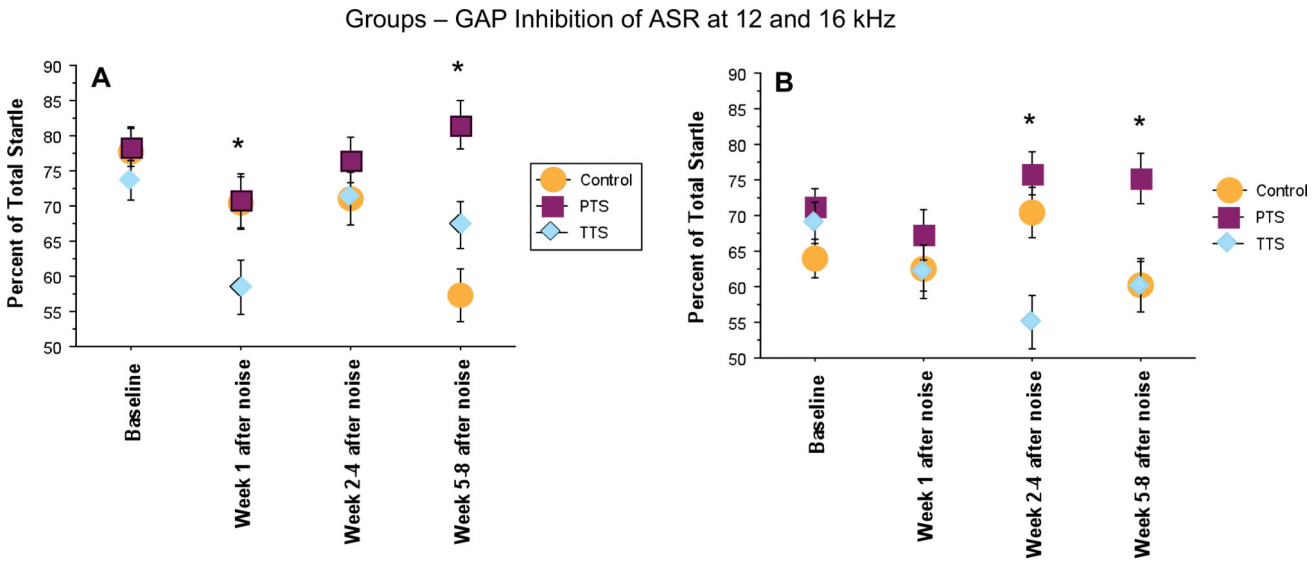

Fig. 6.

Comparisons across groups for GAP inhibition of ASR at 12 and 16 kHz. The PTS group demonstrated a decreased ability to inhibit the ASR 5–8 weeks following noise exposure when compared to the control and TTS groups at both 12 kHz (**a**) and 16 kHz (**b**). Asterisks denote significant differences ($p \leq 0.05$)

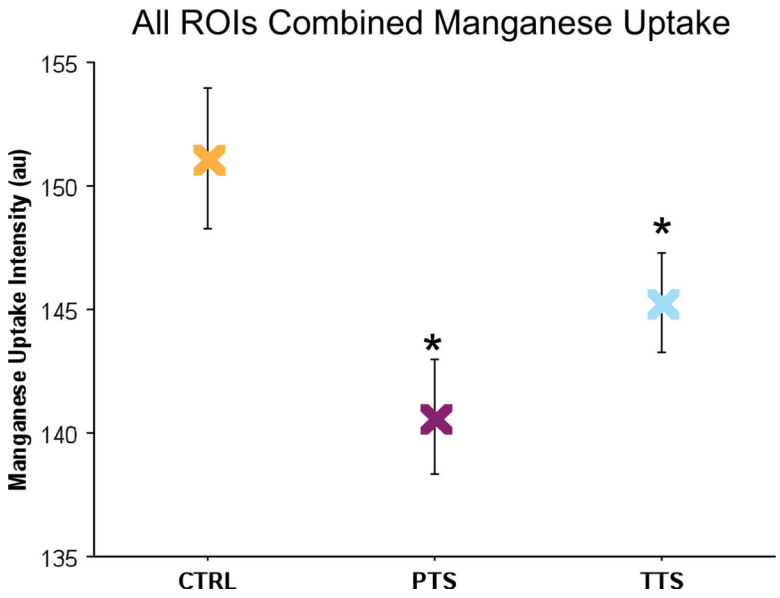

Fig. 7.

Uptake of manganese in the control group was compared with uptake in the PTS and TTS groups 2 months after noise exposure. *au* arbitrary units; asterisks denote significance ($p \leq 0.05$)

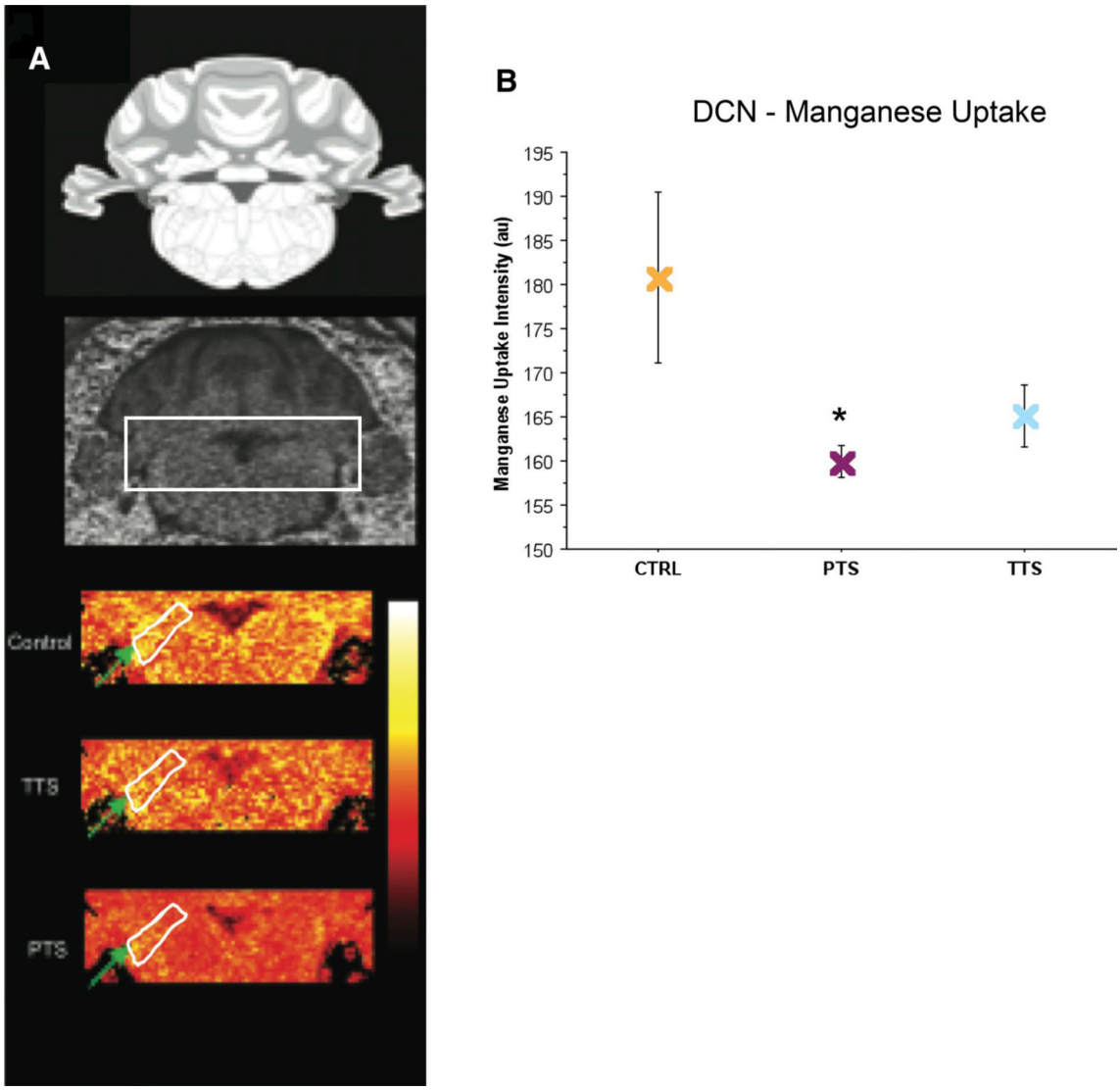

Fig. 8.

Manganese uptake in the dorsal cochlear nucleus (DCN) 2 months following a single noise exposure. **a** A schematic from a rat brain atlas was used as a reference to identify the MRI brain section containing the region of interest. White rectangle on the MRI section is the region enlarged in the representative control, TTS and PTS images. Green arrows designate the region outlined in white under each condition. **b** In the DCN uptake of manganese is significantly diminished in the PTS group 2 months after noise exposure. Error bars: standard error of the mean; *au* arbitrary units; arrows indicate the cochlear nucleus; asterisks denote significance ($p \leq 0.05$)

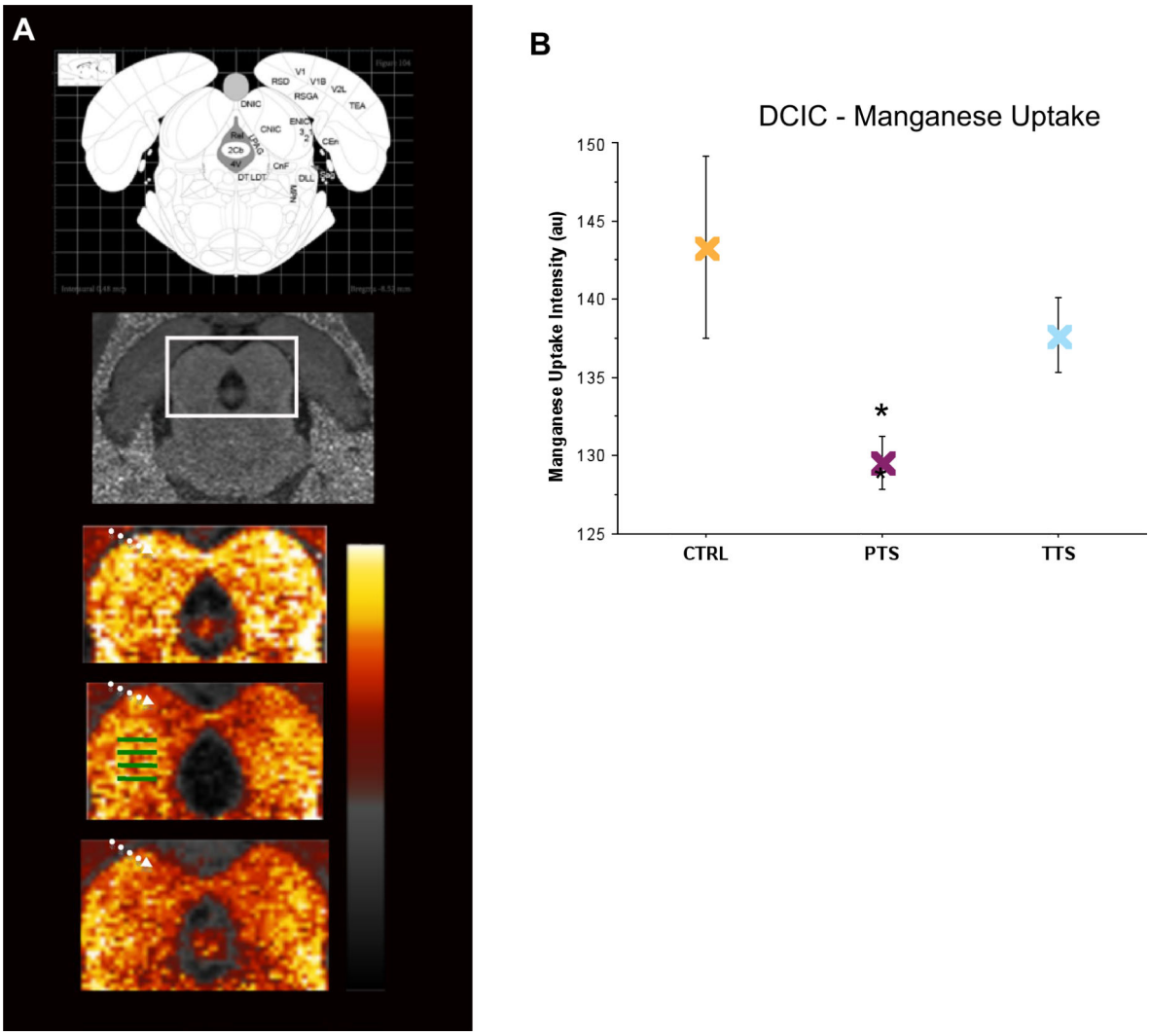

Fig. 9.

Manganese uptake in the dorsal cortex of the inferior colliculus (DCIC) 2 months following a single noise exposure. **a** A schematic from an atlas was used as a reference to identify the MRI brain section containing the region of interest. The white rectangle on the MRI section is the region enlarged in the representative control, PTS, and TTS images. **b** In the DCIC uptake of manganese is significantly diminished in the PTS group 2 months after noise exposure. Error bars: standard error of the mean; *au* arbitrary units; green lines indicate regions within the CIC, from dorsal to ventral—D1, D2, V1, and V2. Arrows indicate the DCIC; asterisk-significance ($p \leq 0.05$)

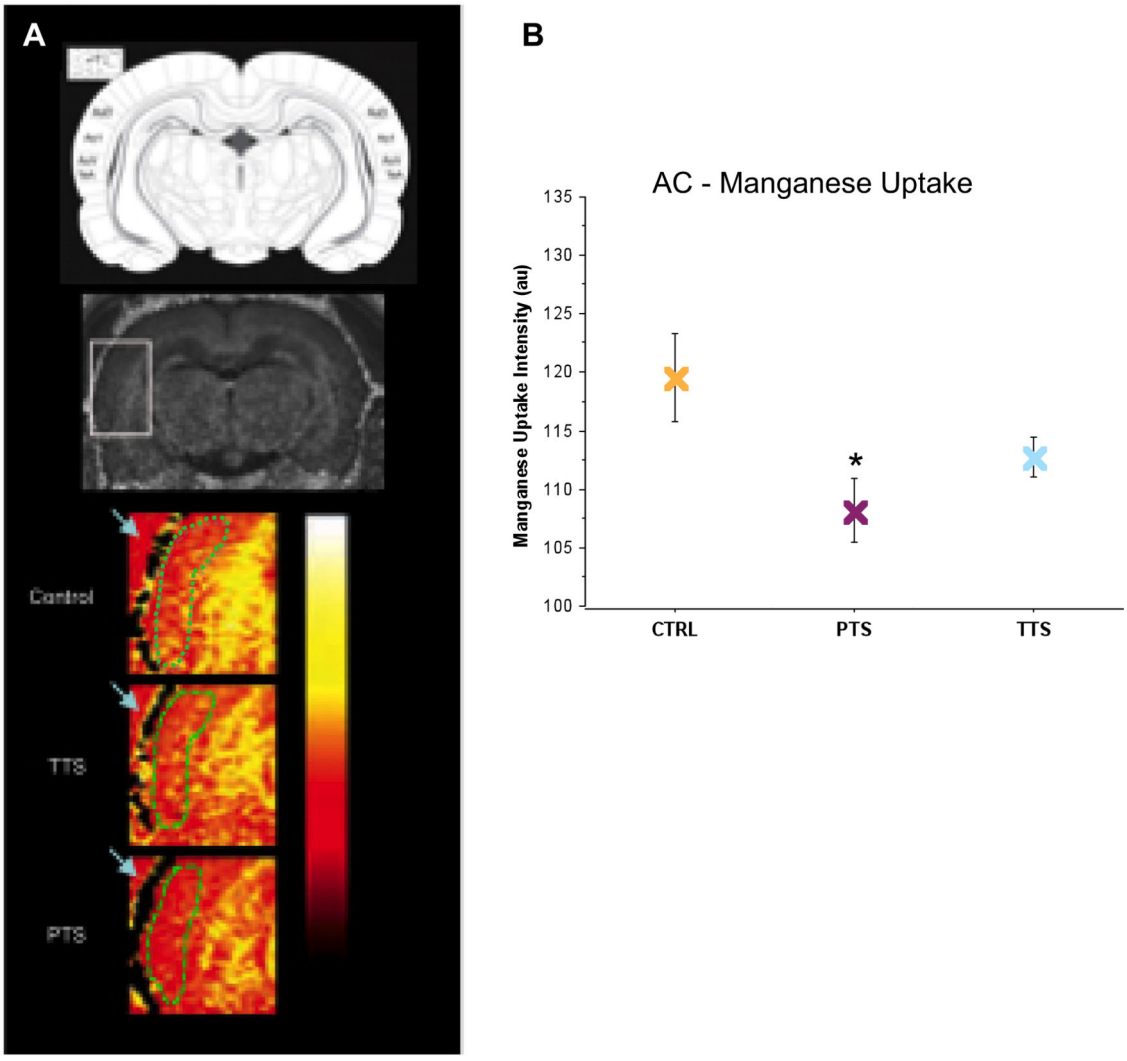

Fig. 10.

Manganese uptake in the auditory cortex (AC) 2 months following a single noise exposure. **a** A schematic from an atlas was used as a reference to identify the MRI brain section containing the region of interest. The white rectangle on the MRI section is the region enlarged in the representative control, PTS, and TTS images. **b** In the AC uptake of manganese is significantly diminished in the PTS group 2 months after noise exposure. Error bars: standard error of the mean; *au* arbitrary units; Green lines outline the AC; arrows indicate muscle; asterisk-significance ($p \leq 0.05$)

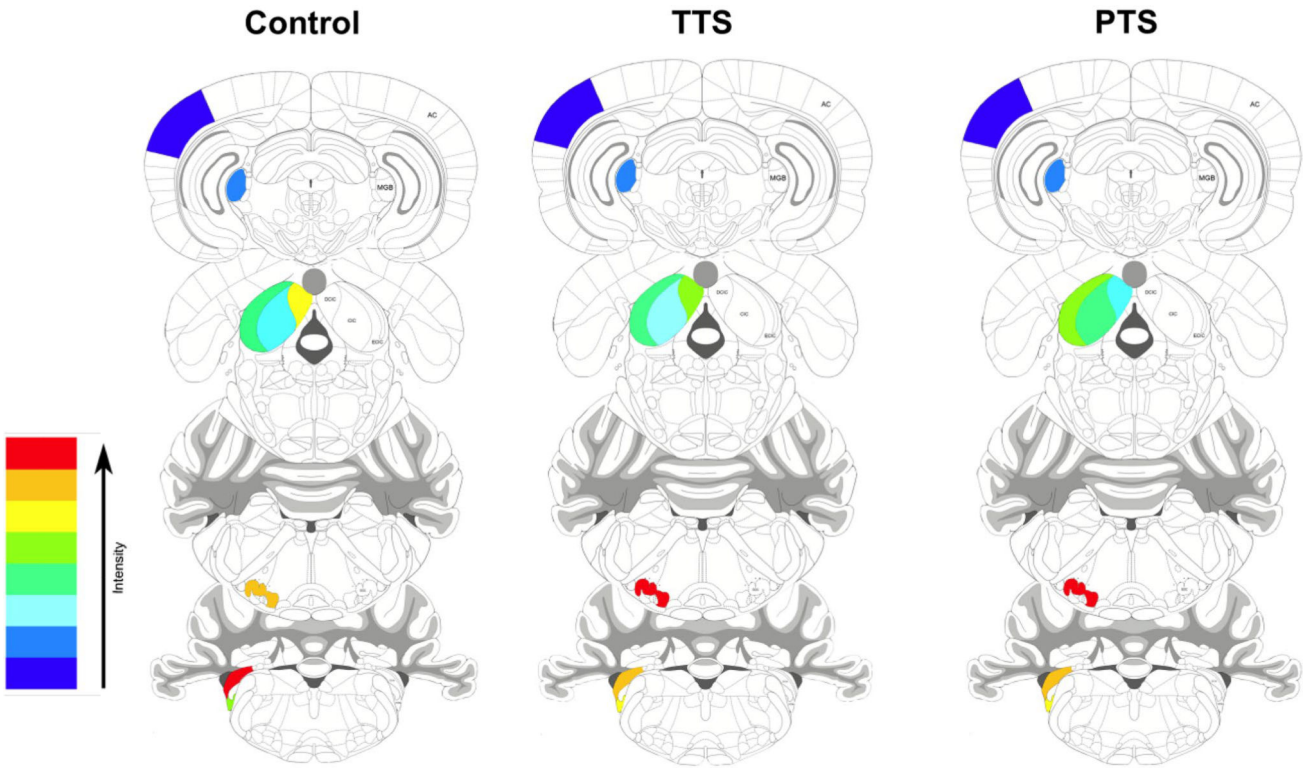

Fig. 11.

Noise exposed normal hearing animals exhibit reorganized neuronal activity maps within auditory pathways. Color scale represents manganese uptake across auditory-related nuclei. Within each group (control, TTS, and PTS) lowest regions of uptake are represented in blue and highest levels of uptake are in red. The top row demonstrates uptake in the AC, and MGB. The second row from the top demonstrates uptake in subdivisions of the IC (CNIC, DCIC, and ECIC). The third row from the top demonstrates uptake in the SOC and the bottom shows manganese uptake in the DCN and VCN

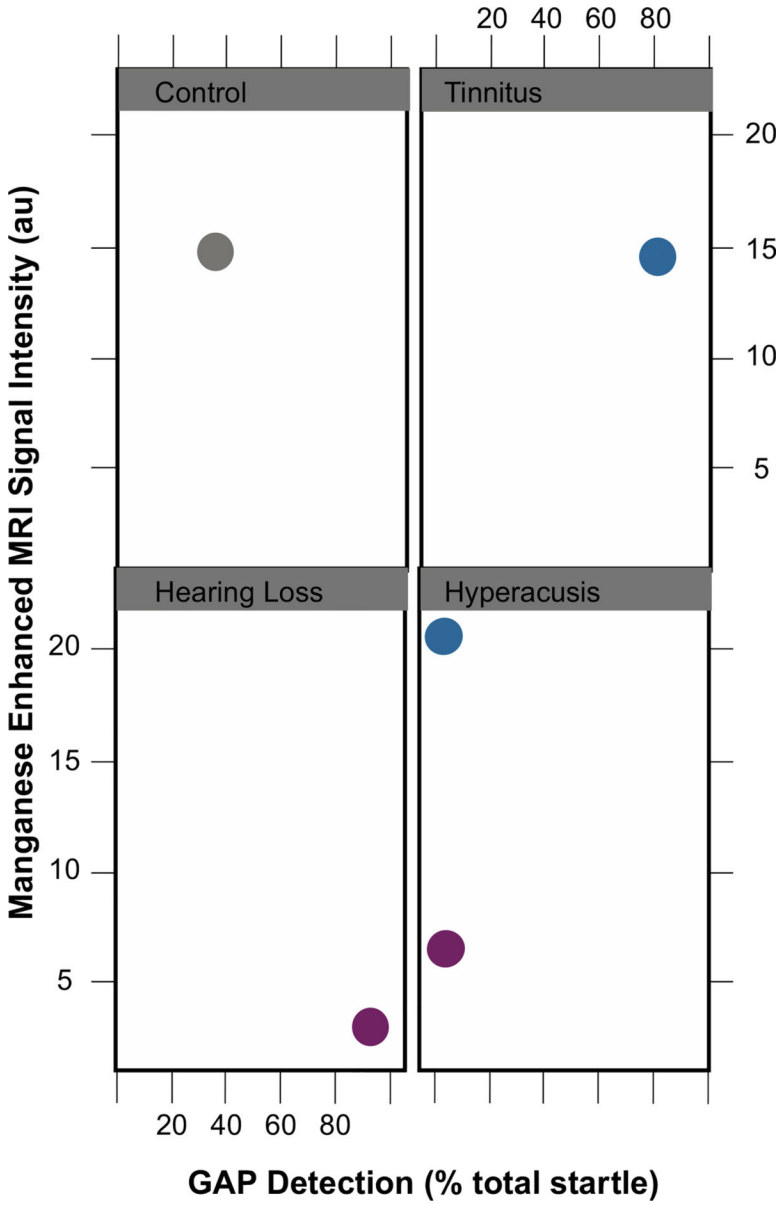

Fig. 12.

Proposed correlation of GAP detection performance with manganese uptake to differentiate tinnitus from hearing loss and hyperacusis. Manganese uptake is represented on the *y*-axis and GAP detection is reflected on the *x*-axis. Dots represent manganese uptake and Gap deterction under control conditions (grey dot), following the onset of tinnitus (blue dot) and after hearing loss (purple dot)

Table 1

Hearing thresholds (dB, SPL) from auditory brainstem responses from normal hearing controls (a) or 2 days and 2 months following noise exposure resulting in either a TTS (b) or a PTS (c)

Treatment groups	Thresholds (dB) 2 days after noise				Thresholds (dB) 2 months after noise			
	Exposed ear		Unexposed ear		Exposed ear		Unexposed ear	
	12 kHz	20 kHz	12 kHz	20 kHz	12 kHz	20 kHz	12 kHz	20 kHz
(a) Control	32	33	30	33	32	33	32	34
(b) TTS	42	41	34	29	34	36	31	32
(c) PTS	64	60	53	50	37	41	32	34

Table 2

Manganese uptake in dorsal and ventral regions of the CIC

	D1	D2	V1	V2
Control[a]	154 ± 5	152 ± 4	150 ± 4	149 ± 6
PTS[b]	138 ± 2	135 + 2	138 ± 1	138 ± 2
TTS[c]	143 ± 7	143 ± 7	142 ± 7	141 ± 8
PTS[b]/control[a]				
Mean % ± error	90 ± 1	89 ± 1	92 ± 1	93 ± 1
p value	0.040	0.016	0.038	0.162
TTS[c]/control[a]				
Mean % ± error	93 ± 5	94 ± 5	95 ± 5	95 ± 5
p value	0.212	0.269	0.315	0.411

The most dorsal sections are D1 followed by D2. The most ventral section is V2 and V1 is positioned just dorsal to V2

[a]Manganese uptake within tonotopic regions of the central nucleus of the inferior colliculus of controlsor

[b]2 months following noise exposure resulting in either a PTS or

[c]a TTS